

# Velocity of Sound beyond the High-Density Relativistic Limit from Lattice Simulation of Dense Two-Color QCD

Kei Iida<sup>1,\*</sup> and Etsuko Itou<sup>2,3,4,†</sup>

<sup>1</sup>*Department of Mathematics and Physics, Kochi University, 2-5-1 Akebono-cho, Kochi 780-8520, Japan*

<sup>2</sup>*Interdisciplinary Theoretical and Mathematical Sciences Program (iTHEMS), RIKEN, Wako 351-0198, Japan*

<sup>3</sup>*Department of Physics, and Research and Education Center for Natural Sciences, Keio University, 4-1-1 Hiyoshi, Yokohama, Kanagawa 223-8521, Japan*

<sup>4</sup>*Research Center for Nuclear Physics (RCNP), Osaka University, Osaka 567-0047, Japan*

(Dated: October 14, 2022)

We obtain the equation of state (EoS) for two-color QCD at low temperature and high density from the lattice Monte Carlo simulation. We find that the velocity of sound exceeds the relativistic limit ( $c_s^2/c^2 = 1/3$ ) after BEC-BCS crossover in the superfluid phase. Such an excess of the sound velocity is previously unknown from any lattice calculations for QCD-like theories. This finding might have a possible relevance to the EoS of neutron star matter revealed by recent measurements of neutron star masses and radii.

The equation of state (EoS) of dense QCD at low temperature is still poorly known but is indispensable particularly because it is related with understanding neutron star observations including recent simultaneous measurements of masses and radii of neutron stars [1–7]. Several early works based on a phenomenological quark-hadron crossover picture of neutron star matter [2, 4] suggested that the zero-temperature sound velocity squared,  $c_s^2 = \partial p / \partial e$ , peaks in the intermediate density region in such a way as to fulfill various observational constraints. Here,  $p$  and  $e$  denote the pressure and internal energy density of the system, respectively. More recently, based on a quarkyonic matter model, McLerran and Reddy [8] have shown that the peak appears slightly above nuclear saturation density. Furthermore, Kojo [9] proposed a microscopic interpretation on the origin of the peak based on a quark saturation mechanism, which is supposed to work for any number of colors. Actually, Kojo and Suenaga [10] indicated that a similar peak of  $c_s^2$  emerges not only in 3-color QCD, but also in 2-color QCD.

The intermediate density regime, which intervenes between the dilute hadron and perturbative QCD (pQCD) regimes, is not analytically accessible. The first-principles calculations of dense QCD have been desired, but not yet been successful because of the severe sign problem. On the other hand, the sign problem is absent in even-flavor dense 2-color QCD because of the pseudo-reality of fundamental quarks.

In the case of 2-color QCD, furthermore, the diquark condensate, which occurs in the superfluid phase, is color singlet. Then we can add an external source term of the diquark condensate to explicitly break the U(1) baryon symmetry as a standard technique to study spontaneous symmetry breaking. It allows us to perform numerical simulations of 2-color QCD in the superfluid phase without any approximation. 2-color QCD at zero chemical potential exhibits the same properties as 3-color QCD, *e.g.*, confinement, spontaneous chiral symmetry breaking, and thermodynamic behaviors. Under these circumstances, it is expected that 2-color QCD even at non-zero chemical potential could be a good testing ground in obtaining qualitative understanding in dense QCD.

Based on this motivation, several Monte Carlo studies on 2-color QCD have been conducted independently and intensively in recent years [11–31]. Putting the results from Refs. [16, 18, 21, 24, 26, 31] together, one can conclude that the 2-color QCD phase diagram is quantitatively clarified. Most remarkably, the emergence of superfluidity at fairly high temperature,  $T \approx 100$  MeV, has been found.

In this work, we numerically obtain the EoS and the sound velocity in dense 2-color QCD. We use the same lattice setup as our previous works [22, 26, 29, 30] and confine ourselves to  $T \approx 79$  MeV, where the hadronic, hadronic-matter, BEC (Bose-Einstein condensed), and BCS phases emerge as density increases. Although first-principles calculations of EoS have been performed in [13, 17, 25, 31], the sound velocity has not yet been examined.

Let us explain our simulation strategy. The lattice gauge action used in this work is the Iwasaki gauge

\* iida(at)kochi-u.ac.jp

† itou(at)yukawa.kyoto-u.ac.jp

action, which is composed of the plaquette term with  $W_{\mu\nu}^{1\times 1}$  and the rectangular term with  $W_{\mu\nu}^{1\times 2}$ ,

$$S_g = \beta \sum_x \left( c_0 \sum_{\substack{\mu < \nu \\ \mu, \nu = 1}}^4 W_{\mu\nu}^{1\times 1}(x) + c_1 \sum_{\substack{\mu \neq \nu \\ \mu, \nu = 1}}^4 W_{\mu\nu}^{1\times 2}(x) \right), \quad (1)$$

where  $\beta = 4/g_0^2$  in the 2-color theory and  $g_0$  denotes the bare gauge coupling constant. Under the normalization condition  $c_0 + 8c_1 = 1$ , the coefficient  $c_1$  is set to  $-0.331$  [32].

The two-flavor fermion action including the quark number operator and the diquark source term is given by

$$S_F = (\bar{\psi}_1 \quad \bar{\varphi}) \begin{pmatrix} \Delta(\mu) & J\gamma_5 \\ -J\gamma_5 & \Delta(-\mu) \end{pmatrix} \begin{pmatrix} \psi_1 \\ \varphi \end{pmatrix} \equiv \bar{\Psi} \mathcal{M} \Psi, \quad (2)$$

where  $\bar{\varphi} = -\psi_2^T C \tau_2$ ,  $\varphi = C^{-1} \tau_2 \bar{\psi}_2^T$ . Here, the indices 1, 2 of  $\psi$  denote the label of the flavor and the  $\Delta(\mu)_{x,y}$  is the Wilson-Dirac operator with the number operator. The additional parameter  $J$  corresponds to the diquark source parameter, which allows us to perform the numerical simulation in the superfluid phase. Note that  $J = j\kappa$ , where  $j$  is a source parameter in the corresponding continuum theory, and  $\kappa$  is the hopping parameter. The  $C$  in  $\bar{\varphi}, \varphi$  is the charge conjugation operator, and  $\tau_2$  acts on the color index. The square of the extended matrix ( $\mathcal{M}$ ) can be diagonal, but  $\det[\mathcal{M}^\dagger \mathcal{M}]$  corresponds to the fermion action for the four-flavor theory, since a single  $\mathcal{M}$  in Eq. (2) represents the fermion kernel of the two-flavor theory. To reduce the number of fermions, we take the root of the extended matrix in the action. In practice, utilizing the Rational Hybrid Monte Carlo (RHMC) algorithm, we can generate gauge configurations.

Now, we utilize a fixed scale method to obtain the EoS at finite density [13]. The trace anomaly can be described by the beta-function of parameters and the trace part of the energy-momentum tensor. In our lattice setup, which is explicitly given by

$$e - 3p = \frac{1}{N_s^3 N_\tau} \left( a \frac{d\beta}{da} \Big|_{\text{LCP}} \left\langle \frac{\partial S}{\partial \beta} \right\rangle_{sub.} + a \frac{d\kappa}{da} \Big|_{\text{LCP}} \left\langle \frac{\partial S}{\partial \kappa} \right\rangle_{sub.} + a \frac{\partial j}{\partial a} \Big|_{\text{LCP}} \left\langle \frac{\partial S}{\partial j} \right\rangle_{sub.} \right). \quad (3)$$

Here,  $a$  is the lattice spacing, and the beta-function for each parameter is evaluated at  $\mu = T = 0$  along

the line of constant physics (LCP). Note that there is no renormalization for the quark number density as it is a conserved quantity. We take all physical observables in the  $j \rightarrow 0$  limit, which implies that the third term in the right side can be eliminated.  $\langle \mathcal{O} \rangle_{sub.}(\mu)$  denotes the subtraction of the vacuum quantity. In this paper, we take  $\langle \mathcal{O} \rangle_{sub.}(\mu) = \langle \mathcal{O}(\mu) \rangle - \langle \mathcal{O}(\mu = 0) \rangle$  at a fixed temperature.

In this work, we perform the simulation with  $(\beta, \kappa, N_s, N_\tau) = (0.80, 0.159, 16, 16)$ . Thanks to the scale setting function (Eq. (23)) and a set of  $(\beta, \kappa)$  with a fixed mass ratio of pseudoscalar and vector mesons  $m_{PS}/m_V$  (Table 1) in Ref. [29], the coefficients can be nonperturbatively determined as  $ad\beta/da|_{\beta=0.80, \kappa=0.159} = -0.352$  and  $ad\kappa/da|_{\beta=0.80, \kappa=0.159} = 0.0282$ .

The pressure can be expressed by the integral of the number density in the thermodynamic limit, namely,  $p(\mu) = \int_{\mu_o}^{\mu} n_q(\mu') d\mu'$ . On the lattice, we perform the numerical integration to obtain  $p(\mu)$ . To reduce the discretization effects, we utilize the following definition proposed in Eq.(29) in Ref. [13]:

$$\frac{p}{p_{SB}}(\mu) = \frac{\int_{\mu_o}^{\mu} d\mu' \frac{n_{SB}^{cont.}(\mu')}{n_q^{tree}} n_q^{latt.}(\mu')}{\int_{\mu_o}^{\mu} d\mu' n_{SB}^{cont.}(\mu')}, \quad (4)$$

in which the lattice numerical data ( $n_q^{latt.}(\mu)$ ) are normalized by the quark number density on the same lattice spacing  $n_q^{tree}$  which is analytically calculated by the free field propagator on the finite lattice (See Eq. (26) in Ref. [13]). Here, we numerically calculate  $n_q^{latt.} \equiv a^3 n_q = \sum_i \kappa \langle \bar{\psi}_i(x) (\gamma_0 - \mathbb{I}_4) e^{\mu U_4(x)} \psi_i(x + \hat{4}) + \bar{\psi}_i(x) (\gamma_0 + \mathbb{I}_4) e^{-\mu U_4^\dagger(x - \hat{4})} \psi_i(x - \hat{4}) \rangle$ . Furthermore, to reduce the discretization effect of the numerical integration, we take the ratio between  $p(\mu)$  and its value at the Stefan-Boltzman (SB) limit ( $p_{SB}(\mu)$ ) which is also obtained by the numerical integration of the number density of quarks in the relativistic limit, namely  $n_{SB}^{cont.} = N_f N_c (\mu T^2 + \mu^3/\pi^2)/3$ , where  $N_f$  ( $N_c$ ) is the number of flavors (colors). In (4),  $\mu_o$  represents the onset scale, namely, the starting point at which  $\langle n_q \rangle$  becomes nonzero as  $\mu$  increases. In the continuum theory, the pressure scales as  $p_{SB}(\mu) = \int^{\mu} n_{SB}^{cont.}(\mu') d\mu' \approx N_f N_c \mu^4 / (12\pi^2)$  in the high  $\mu$  regime.

To study the EoS and the sound velocity, we have increased the number of the values of  $a\mu$  at intervals of  $a\Delta\mu = 0.05$  and also accumulated statistics (100–300 configurations) since the previous paper [26]. The statistical errors are estimated by the jackknife analysis. According to Ref. [29], once we

introduce the physical scale as  $T_c = 200$  MeV, where  $T_c$  denotes the pseudo-critical temperature of chiral phase transition at  $\mu = 0$ , then our parameter set,  $\beta = 0.80$  and  $N_\tau = 16$  ( $T = 0.39T_c$ ), corresponds to  $a \approx 0.17$  fm and  $T \approx 79$  MeV. The mass of lightest pseudo-scalar (PS) meson at  $\mu = 0$ ,  $m_{PS}$ , is still heavy in our simulations,  $am_{PS} = 0.6229(34)$  ( $m_{PS} \approx 750$  MeV).

We show the schematic picture of the phase structure in Fig. 1 and summarize the definition of each phase in Table I, which is an extract from Ref. [26].

The order parameters that help classify the phases

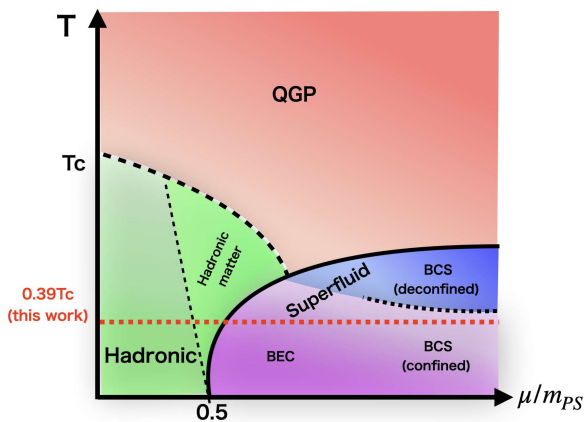


FIG. 1. Schematic 2-color QCD phase diagram. Each phase is defined in Table I.

	Hadronic		Superfluid	
	Hadronic matter	BEC	BCS	BCS
$\langle  L  \rangle$	zero	zero	non-zero	non-zero
$\langle qq \rangle$	zero	zero	non-zero	non-zero
$\langle n_q \rangle$	zero	non-zero	$0 < \frac{\langle n_q^{latt.} \rangle}{n_q^{tree}} < 1$	$\frac{\langle n_q^{latt.} \rangle}{n_q^{tree}} \approx 1$

TABLE I. Definition of phases.

are the Polyakov loop  $\langle |L| \rangle$  and diquark condensate  $\langle qq \rangle$ , whose zero/nonzero values indicate the confinement and the superfluidity, respectively. We found that the superfluidity emerges at  $\mu_c/m_{PS} \approx 0.5$  as expected by the chiral perturbation theory (ChPT) [33]. It is natural to use  $\mu/m_{PS}$  as a dimensionless parameter of density since the critical value  $\mu_c$  can be approximated by  $m_{PS}/2$  even if the value of  $m_{PS}$  in numerical simulation would be changed [34]. We also confirmed that the scaling law of the order parameter around it is consistent

with the ChPT prediction. Furthermore, we measured the quark number operator  $\langle n_q^{latt.} \rangle$ . We identified the regime where  $\langle n_q^{latt.} \rangle$  is consistent with the free quark theory as the BCS phase (See Fig.7 in Ref. [26]). Thus, we concluded that there are hadronic, hadronic-matter, BEC and BCS phases at  $T = 79$  MeV, although there is no clear boundary between the BEC and BCS phases. Interestingly, up to  $\mu/m_{PS} = 1.28$  ( $\mu \lesssim 960$  MeV), the confining behavior remains, while nontrivial instanton configurations have been discovered from calculations of the topological susceptibility [26]. It indicates that a naive perturbative picture, for instance, pQCD, is not yet valid in the density regime studied here.

The trace anomaly and pressure are shown in Fig. 2. For the trace anomaly, we plot the gauge part (the first term in Eq. (3)) and minus the fermion part (the second term) separately. Both parts are normalized by  $\mu^4$  to see the dimensionless asymptotic behavior. The magnitude of each part has a peak around the hadronic-superfluid phase transition. It is very similar to the emergence of the peak of  $(e-3p)/T^4$  around the hadronic-QGP phase transition at  $\mu = 0$ .

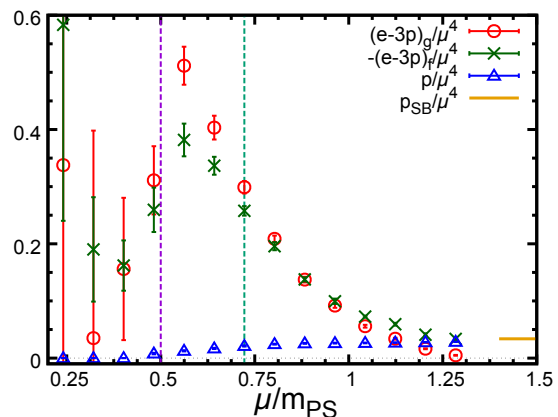


FIG. 2. Trace anomaly and pressure as a function of  $\mu/m_{PS}$ . The circle and cross symbols denote the gauge part and *minus* the fermion part of the trace anomaly, respectively. We also show  $p/\mu^4$  at the relativistic limit,  $p_{SB}/\mu^4 = N_f N_c / (12\pi^2)$ . The purple dashed line denotes the critical value,  $\mu_c$ , which is the hadronic-superfluid phase transition point, while the green dashed line indicates that the BEC-BCS crossover occurs around this value of  $\mu$ .

As for the pressure, at  $\mu_c = m_{PS}/2$  for the hadronic-superfluid phase transition (purple vertical line),  $p$  takes a non-zero value since  $\langle n_q \rangle$  becomes

non-zero in the hadronic-matter phase. Thus,  $\langle n_q \rangle$  becomes non-zero before the hadronic-superfluid phase transition, then  $\mu_c$  is not the same as  $\mu_o$  in Eq. (4). The low but finite temperature effects cause the discrepancy between them as discussed in [26]. We can see that our data monotonically increase and approach the value in the relativistic limit. The value of  $p/p_{SB}$  is  $\approx 0.84$  at the highest density in our simulation.

Combining the data of  $e - 3p$  and  $p$  above, we finally obtain the EoS and sound velocity as shown in the top and bottom panels of Fig. 3, respectively. In

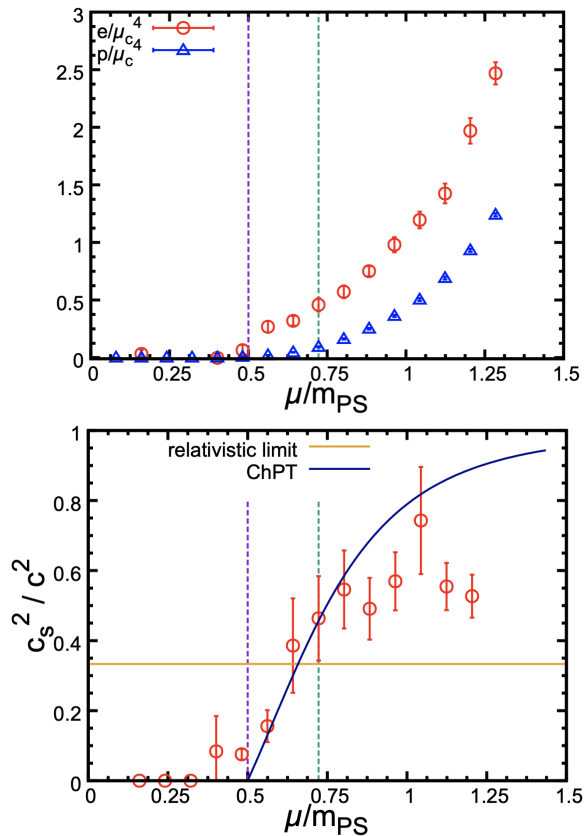


FIG. 3. Top: The EoS as a function of  $\mu/m_{PS}$ . Bottom: Sound velocity squared as a function of  $\mu/m_{PS}$ . The horizontal line (orange) denotes the value in the relativistic limit,  $c_s^2/c^2 = 1/3$ . The blue curve shows the result of ChPT.

the top panel, we normalize  $e$  and  $p$  by  $\mu_c$  so as to be dimensionless. We can see that both  $e$  and  $p$  are consistent with zero in the hadronic phase. Thus, these thermodynamic quantities are not changed even if  $\mu$  increases before the hadronic-superfluid phase transition.

Now, let us focus on the sound velocity depicted in the bottom panel in Fig. 3. Here, we evaluate  $c_s^2(\mu) = \Delta p(\mu)/\Delta e(\mu)$ , where  $\Delta p(\mu)$  and  $\Delta e(\mu)$  are estimated by the symmetric finite difference, i.e.,  $\Delta p(\mu) = (p(\mu + \Delta\mu) - p(\mu - \Delta\mu))/2$ . First of all, our results are consistent with the prediction of ChPT [13, 35], which is given by  $c_s^2/c^2 = (1 - \mu_c^4/\mu^4)/(1 + 3\mu_c^4/\mu^4)$ , in the BEC phase. According to Ref. [35], the prediction of ChPT is valid in a low  $\mu$  regime where  $\mu$  is smaller than  $m_V$ . Furthermore, the quark mass is still heavy in our simulations. To find the reason why ChPT shows such a nice consistency with the lattice data will be interesting future work not only in the context of EoS but also in the context of mass spectrum [36–38]. We also find that  $c_s^2/c^2$  is larger than  $1/3$ , which is the value in the relativistic limit, at higher densities than the regime where the BEC-BCS crossover occurs. Eventually, our data seem to peak around  $\mu \approx m_{PS}$  and, as density increases further, decrease so as to go away from the ChPT prediction. *Such a peak of the sound velocity is a characteristic feature previously unknown from any lattice calculations for QCD-like theories.* For example, in the finite temperature case, the sound velocity monotonically increases in  $T > T_c$  and approaches the relativistic limit as the temperature increases [39, 40].

It is strongly believed that at ultrahigh density,  $c_s^2/c^2$  approaches the relativistic limit. Then, there arises a question of *how* it approaches  $1/3$ . According to the pQCD analysis (see Appendix A in [7]), it scales as  $c_s^2/c^2 \approx (1 - 5\beta_0\alpha_s^2/(48\pi^2))/3$ , where  $\beta_0 = (11N_c - 2N_f)/3$  denotes the 1-loop coefficient of the beta-function. Thus,  $c_s^2/c^2$  approaches the asymptotic value from *below*. On the other hand, a result based on the resummed perturbation theory suggests that  $c_s^2/c^2$  approaches the limit from *above* [41]. In the numerical simulations, the maximum value of  $\mu$  is limited by  $\mu \ll 1/a$  to avoid the strong lattice artefact. Otherwise, the hopping term of fermions would be partially suppressed by the factor  $e^{-a\mu}$  in the Wilson-Dirac operator. For the extension to larger chemical potential, we need to perform the smaller lattice spacing or lighter quark mass simulations. Furthermore, to obtain  $c_s$  at  $T = 0$ , it is also required to see the EoS in the lower temperature regime by carrying out the larger volume simulations.

According to Ref. [9], a peak of  $c_s^2$  appears due to the development of the quark Fermi sea just after the saturation of low momentum quarks. The density at

which the peak appears in our results is apparently low, i.e.,  $\mu \approx m_{PS}$ , but seems sufficiently high that the quark Fermi sea would be fully developed. It supports the predictions from several effective models based on the presence of the quark Fermi sea [8–10]. Furthermore, it is reported that the peak of sound velocity emerges around BEC-BCS crossover also in condensed matter systems with finite-range interactions [42]. To ask whether or not the emergence of the peak structure is a universal property of superfluids in a BEC-BCS crossover regime, it would be important to investigate the origin of this structure as another future work. If the peak of sound velocity would be a universal property even for real 3-color QCD as discussed in Refs. [9, 10], then it will change one of the conventional pictures that explain the presence of massive neutron stars, namely, a first order transition from stiffened hadronic matter to soft quark matter.

## ACKNOWLEDGMENTS

We would like to thank T. Hatsuda, T. Kojo, T. Saito, D. Suenaga, H. Tajima and H. Togashi for useful conversations. We are grateful to S. Hands and J.-I. Skullerud for calling our attention to erroneous data in the earlier version of the manuscript. The consistency with ChPT was kindly suggested by N. Yamamoto. E. I. especially thanks T. Kojo T. Hatsuda and H. Togashi for fruitful discussions about the origin of peak, the pQCD analysis and the correspondence between the lattice data and neutron-matter analysis. Discussions in the working group “Gravitational Wave and Equation of State” in iTHEMS, RIKEN was useful for completing this work. The work of E. I. is supported by JSPS KAKENHI with Grant Number 19K03875, JST PRESTO Grant Number JPMJPR2113 and JSPS Grant-in-Aid for Transformative Research Areas (A) JP21H05190, and the work of K. I. is supported by JSPS KAKENHI with Grant Numbers 18H05406 and 18H01211. The numerical simulation is supported by the HPCI-JHPCN System Research Project (Project ID: jh220021).

- 
- [1] M. G. Alford, A. Schmitt, K. Rajagopal, and T. Schäfer, “Color superconductivity in dense quark matter,” *Rev. Mod. Phys.* **80** (2008) 1455–1515, [arXiv:0709.4635 \[hep-ph\]](#).
- [2] K. Masuda, T. Hatsuda, and T. Takatsuka, “Hadron–quark crossover and massive hybrid stars,” *Prog Theor Exp Phys* **2013** no. 7, (July, 2013) 073D01.
- [3] A. L. Watts, N. Andersson, D. Chakrabarty, M. Feroci, K. Hebeler, G. Israel, F. K. Lamb, M. C. Miller, S. Morsink, F. Özel, A. Patruno, J. Poutanen, D. Psaltis, A. Schwenk, A. W. Steiner, L. Stella, L. Tolos, and M. van der Klis, “Colloquium: Measuring the neutron star equation of state using x-ray timing,” *Rev. Mod. Phys.* **88** no. 2, (Apr., 2016) 021001.
- [4] G. Baym, T. Hatsuda, T. Kojo, P. D. Powell, Y. Song, and T. Takatsuka, “From hadrons to quarks in neutron stars: a review,” *Rept. Prog. Phys.* **81** no. 5, (2018) 056902, [arXiv:1707.04966 \[astro-ph.HE\]](#).
- [5] **LIGO Scientific, Virgo** Collaboration, B. P. Abbott *et al.*, “GW170817: Measurements of neutron star radii and equation of state,” *Phys. Rev. Lett.* **121** no. 16, (2018) 161101, [arXiv:1805.11581 \[gr-qc\]](#).
- [6] S. Huth *et al.*, “Constraining Neutron-Star Matter with Microscopic and Macroscopic Collisions,” *Nature (London)* **606** (2022) 276–280, [arXiv:2107.06229 \[nucl-th\]](#).
- [7] T. Kojo, G. Baym, and T. Hatsuda, “QHC21 equation of state of neutron star matter – in light of 2021 NICER data,” [arXiv:2111.11919 \[astro-ph.HE\]](#).
- [8] L. McLerran and S. Reddy, “Quarkyonic matter and neutron stars,” *Phys. Rev. Lett.* **122** no. 12, (Mar., 2019) 122701.
- [9] T. Kojo, “Stiffening of matter in quark-hadron continuity,” *Phys. Rev. D* **104** no. 7, (2021) 074005, [arXiv:2106.06687 \[nucl-th\]](#).
- [10] T. Kojo and D. Suenaga, “Peaks of sound velocity in two color dense QCD: quark saturation effects and semishort range correlations,” *Phys. Rev. D* **105** no. 7, (2022) 076001, [arXiv:2110.02100 \[hep-ph\]](#).
- [11] S. Muroya, A. Nakamura, and C. Nonaka, “Study of the finite density state based on SU(2) lattice QCD,” *Nucl. Phys. B Proc. Suppl.* **119** (2003) 544–546, [arXiv:hep-lat/0208006](#).
- [12] S. Muroya, A. Nakamura, and C. Nonaka, “Behavior of hadrons at finite density – lattice study of color SU(2) QCD,” *Phys. Lett. B* **551**

- (2003) 305–310, [arXiv:hep-lat/0211010](#).
- [13] S. Hands, S. Kim, and J.-I. Skullerud, “Deconfinement in dense 2-color QCD,” *Eur. Phys. J. C* **48** (2006) 193, [arXiv:hep-lat/0604004](#).
- [14] S. Hands, P. Sitch, and J.-I. Skullerud, “Hadron spectrum in a Two-Colour Baryon-Rich medium,” *Phys. Lett. B* **662** (2008) 405–412, [arXiv:0710.1966 \[hep-lat\]](#).
- [15] S. Hands and P. Kenny, “Topological fluctuations in dense matter with two colors,” *Phys. Lett. B* **701** (2011) 373–377, [arXiv:1104.0522 \[hep-lat\]](#).
- [16] S. Cotter, P. Giudice, S. Hands, and J.-I. Skullerud, “Towards the phase diagram of dense two-color matter,” *Phys. Rev. D* **87** no. 3, (2013) 034507, [arXiv:1210.4496 \[hep-lat\]](#).
- [17] S. Hands, S. Cotter, P. Giudice, and J.-I. Skullerud, “The phase diagram of two color QCD,” *J. Phys. Conf. Ser.* **432** (2013) 012020, [arXiv:1210.6559 \[hep-lat\]](#).
- [18] S. Cotter, J.-I. Skullerud, P. Giudice, S. Hands, S. Kim, and D. Mehta, “Phase structure of QC2D at high temperature and density,” *PoS LATTICE2012* (2012) 091, [arXiv:1210.6757 \[hep-lat\]](#).
- [19] T. Boz, S. Cotter, L. Fister, D. Mehta, and J.-I. Skullerud, “Phase transitions and gluodynamics in 2-colour matter at high density,” *Eur. Phys. J. A* **49** (2013) 87, [arXiv:1303.3223 \[hep-lat\]](#).
- [20] T. Boz, P. Giudice, S. Hands, J.-I. Skullerud, and A. G. Williams, “Two-color QCD at high density,” *AIP Conf. Proc.* **1701** no. 1, (2016) 060019, [arXiv:1502.01219 \[hep-lat\]](#).
- [21] V. V. Braguta, E.-M. Ilgenfritz, A. Yu. Kotov, A. V. Molochkov, and A. A. Nikolaev, “Study of the phase diagram of dense two-color QCD within lattice simulation,” *Phys. Rev. D* **94** no. 11, (2016) 114510, [arXiv:1605.04090 \[hep-lat\]](#).
- [22] E. Itou, K. Iida, and T.-G. Lee, “Topology of two-color QCD at low temperature and high density,” *PoS LATTICE2018* (2018) 168, [arXiv:1810.12477 \[hep-lat\]](#).
- [23] N. Y. Astrakhantsev, V. G. Bornyakov, V. V. Braguta, E. M. Ilgenfritz, A. Y. Kotov, A. A. Nikolaev, and A. Rothkopf, “Lattice study of static quark-antiquark interactions in dense quark matter,” *JHEP* **05** (2019) 171, [arXiv:1808.06466 \[hep-lat\]](#).
- [24] T. Boz, P. Giudice, S. Hands, and J.-I. Skullerud, “Dense 2-color QCD towards continuum and chiral limits,” *Phys. Rev. D* **101** no. 7, (2020) 074506, [arXiv:1912.10975 \[hep-lat\]](#).
- [25] T. Boz, P. Giudice, S. Hands, and J.-I. Skullerud, “Dense two-color QCD towards continuum and chiral limits,” *Phys. Rev. D* **101** (Dec., 2019) 074506.
- [26] K. Iida, E. Itou, and T.-G. Lee, “Two-colour QCD phases and the topology at low temperature and high density,” *JHEP* **01** (2020) 181, [arXiv:1910.07872 \[hep-lat\]](#).
- [27] N. Astrakhantsev, V. V. Braguta, E.-M. Ilgenfritz, A. Yu. Kotov, and A. A. Nikolaev, “Lattice study of thermodynamic properties of dense QC<sub>2</sub>D,” *Phys. Rev. D* **102** no. 7, (2020) 074507, [arXiv:2007.07640 \[hep-lat\]](#).
- [28] P. V. Buividovich, D. Smith, and L. von Smekal, “Electric conductivity in finite-density SU(2) lattice gauge theory with dynamical fermions,” *Phys. Rev. D* **102** no. 9, (2020) 094510, [arXiv:2007.05639 \[hep-lat\]](#).
- [29] K. Iida, E. Itou, and T.-G. Lee, “Relative scale setting for two-color QCD with  $N_f=2$  Wilson fermions,” *PTEP* **2021** no. 1, (2021) 013B05, [arXiv:2008.06322 \[hep-lat\]](#).
- [30] K. Ishiguro, K. Iida, and E. Itou, “Flux tube profiles in two-color QCD at low temperature and high density,” in *38th International Symposium on Lattice Field Theory*. 11, 2021. [arXiv:2111.13067 \[hep-lat\]](#).
- [31] V. G. Bornyakov, N. V. Gerasimeniuk, V. A. Goy, A. Nakamura, and R. N. Rogalyov, “Study of two color QCD on large lattices,” *Phys. Rev. D* **105** no. 11, (2022) 114505, [arXiv:2203.04909 \[hep-lat\]](#).
- [32] Y. Iwasaki, “Renormalization Group Analysis of Lattice Theories and Improved Lattice Action. II. Four-dimensional non-Abelian SU(N) gauge model,” [arXiv:1111.7054 \[hep-lat\]](#).
- [33] J. B. Kogut, M. A. Stephanov, D. Toublan, J. J. M. Verbaarschot, and A. Zhitnitsky, “QCD-like theories at finite baryon density,” *Nucl. Phys. B* **582** (2000) 477–513, [arXiv:hep-ph/0001171](#).
- [34] It is expected that the corresponding critical value of  $\mu$  would be  $\mu_c/m_N \approx 1/3$  if the hadronic-superfluid phase transition occurs also in the case of 3-color QCD, where  $m_N$  denotes the nucleon mass.
- [35] D. T. Son and M. A. Stephanov, “QCD at a finite isospin density: From the pion to quark-antiquark condensation,” *Physics of Atomic Nuclei* **64** no. 5, (May, 2001) 834–842. <https://doi.org/10.1134/2F1.1378872>.
- [36] S. Hands, P. Sitch, and J.-I. Skullerud, “Hadron Spectrum in a Two-Colour Baryon-Rich Medium,” *Phys. Lett. B* **662** (2008) 405–412, [arXiv:0710.1966 \[hep-lat\]](#).
- [37] J. Wilhelm, L. Holicki, D. Smith, B. Wellegehausen, and L. von Smekal, “Continuum Goldstone spectrum of two-color QCD at finite density with staggered quarks,” *Phys. Rev. D* **100** no. 11, (2019) 114507, [arXiv:1910.04495 \[hep-lat\]](#).

- [38] K. Murakami, D. Suenaga, K. Iida, and E. Itou, “Measurement of hadron masses in 2-color finite density QCD,” to appear in Proceedings of Lattice 2022.
- [39] S. Borsanyi, Z. Fodor, C. Hoelbling, S. D. Katz, S. Krieg, and K. K. Szabo, “Full result for the QCD equation of state with 2+1 flavors,” *Phys. Lett. B* **730** (2014) 99–104, [arXiv:1309.5258](#) [[hep-lat](#)].
- [40] **HotQCD** Collaboration, A. Bazavov *et al.*, “Equation of state in ( 2+1 )-flavor QCD,” *Phys. Rev. D* **90** (2014) 094503, [arXiv:1407.6387](#) [[hep-lat](#)].
- [41] Y. Fujimoto and K. Fukushima, “Equation of state of cold and dense QCD matter in resummed perturbation theory,” *Phys. Rev. D* **105** no. 1, (2022) 014025, [arXiv:2011.10891](#) [[hep-ph](#)].
- [42] H. Tajima and H. Liang, “Role of the effective range in the density-induced bec-bcs crossover,” *Phys. Rev. A* **106** (Oct, 2022) 043308.